Supporting Information

Multi-Reference Ab Initio Study of the Ground and Low-lying Excited States of $Cr(CO)_2$ and $Cr(CO)_3$

Joonghan Kim,[1,*] Jeongho Kim,[2] and Hyotcherl Ihee[3,4,*]

[1]*Department of Chemistry, The Catholic University of Korea, Bucheon, 420-743, Republic of Korea*

[2]*Department of Chemistry, Inha University, Incheon, 402-751, Republic of Korea*

[3]*Center for Nanomaterials and Chemical Reactions, Institute for Basic Science, Daejeon, 305-701, Republic of Korea*

[4]*Department of Chemistry, KAIST, Daejeon, 305-701, Republic of Korea*

*Corresponding Author

E-mail: joonghankim@catholic.ac.kr and hyotcherl.ihee@kaist.ac.kr

Electron Affinity of CO molecule

An experimental study on endothermic ion-molecule reaction showed that the electron affinity (EA) of CO is 1.37 eV.[1] However, in the NIST webbook webpage,[2] all theoretical methods give negative EA values for CO, indicating that CO^{-} lies higher in energy than CO. To address this discrepancy, Lee *et al.* carefully studied the EA of CO using multi-reference configuration interaction (MRCI) and obtained a negative EA value (–1.67 eV),[3] which is similar to another experimental value (–1.5 eV) obtained from electron scattering.[4] In addition, considering that the EA of N_2, which is isoelectronic with CO^{-}, is negative, they concluded that the positive EA obtained from the experiment is erroneous and the EA of CO is negative.[3]

To examine on our own that the EA of CO is negative, we also calculated the EA of CO using CASPT2 with ANO-RCC-TZ and -QZ basis sets. The active orbitals contain 2*s* and 2*p* orbitals of C and O, thereby CAS(10,8) and CAS(11,8) were used for CO and CO^{-} molecules, respectively. The ground states of CO and CO^{-} are the $^1\Sigma^+$ and $^2\Pi$ states, respectively. Therefore, CASPT2 and MS-CASPT2 (based on SA2-CAS(11,8) wave function) were employed to calculate the electronic states of CO and CO^{-}, respectively. To calculate adiabatic EA of CO, the geometry optimizations of CO and CO^{-} were performed. The zero-point energies calculated by PBE0/aug-cc-pVTZ and PBE0/aug-cc-pVQZ were added for calculating adiabatic EA (We also performed the same calculations using M06 functional. No difference from PBE0 is observed.). The results are listed in Table S1.

As shown in Table S1, the bond length of CO (1.129 Å) calculated by CASPT2 is in excellent agreement with the experimental value (1.128 Å). The bond length of CO^{-} (1.220 Å) optimized by MS-CASPT2/ANO-RCC-QZ is very close to that (1.210 Å) calculated by MRCI. In the calculations of EA, CASPT2 with the triple zeta level of basis set (−2.04 eV) overestimates the magnitude of EA compared with MRCI (−1.67 eV). The improvement of basis sets to quadruple level reduces the magnitude of EA (−1.91 eV). It is noteworthy that the size of basis sets used in the previous MRCI calculations is very large because they contain three additional diffuse *p* basis functions for more accurate calculation of EA. Therefore, the EA of CO calculated by CASPT2/ANO-RCC-QZ is very reasonable in a cost-effective manner.

Computational Details for DFT and MP2

A single-reference method, MP2,[5,6] was used to examine the lack of multiconfigurational character in the ab initio calculations. We used PBE0,[7] M06,[8] and M06-L[9] functionals as an exchange-correlation DFT functional. These DFT functionals have not been used in the previous study.[10] The ultrafine grid for the numerical integration of exchange-correlation functional was used in all the DFT calculations. In the single-reference calculations, the restricted and unrestricted formalisms were used for the singlet and all other spin states, respectively. In MP2 and DFT calculations, we used the AVQZ,[11] [9*s*8*p*6*d*4*f*3*g*2*h*] and AVTZ, [5*s*4*p*3*d*2*f*] for Cr and other atoms (C and O), respectively. The geometry optimizations and subsequent harmonic vibrational frequency calculations were performed using MP2 and DFT methods. All MP2 and DFT calculations were performed using the Gaussian09 program.[12]

Molecular Structure and Energetics of $Cr(CO)_2$ and $Cr(CO)_3$

No experimental values of geometrical parameters of $Cr(CO)_2$ and $Cr(CO)_3$ are available. We assume that the geometrical parameters obtained by CASPT2 are more reliable because only CASPT2 reasonably treat both dynamic and non-dynamic correlation effects. To examine the difference in the optimized geometrical parameters depending on the calculation method, we compare the results of DFT, MP2, and CASSCF with those of CASPT2. First, we note that no DFT functional provides all of the geometrical parameters comparable with those calculated by CASPT2. For example, for the $^3A_2$ and $^5A_1$ states of $Cr(CO)_2$ with bent structures, PBE0 reasonably describes only Cr□C and C□O bond lengths and overestimates the C□Cr□C bond angles compared with those calculated by CASPT2 (see Table S1). When using M06 functional, the C□Cr□C bond angles are similar to those of CASPT2, but the Cr□C bond lengths are overestimated. A single-reference ab initio method cannot give reasonable geometrical parameters of $Cr(CO)_2$, either. As can be seen in Table S1, MP2 seriously overestimates the Cr□C bond lengths of the $^3A_2$ and $^5A_1$ states in comparison with those of CASPT2. In addition, MP2 overestimates the C□Cr□C bond angle of the $^5A_1$ state. These results can be ascribed to the lack of non-dynamic correlation effect in MP2 methods. The comparison between CAS(10,12) and CASPT2 shows that the lack of dynamic correlation in the CASSCF method leads to short Cr□C and long C□O bond lengths and different C□Cr□C bond angles in the bent $^3A_2$ and $^5A_1$ states. The discrepancy between the CASPT2 and other methods is also observed for linear $^5\Pi_g$ and $^7\Pi_u$ states. As shown in Table S1, all DFT methods overestimate the Cr□C bond lengths of the $^5\Pi_g$ and $^7\Pi_u$ states compared

with CASPT2. Also, the comparison between the results of CAS(10,12) and MS-CASPT2 shows that the lack of dynamic correlation in CASSCF significantly affects all the bond lengths of the linear structures of $Cr(CO)_2$. Therefore, in order to obtain accurate molecular structure of transition metal carbonyl complex, it is crucial to consider both non-dynamic and dynamic correlation effects.

No functional used for DFT calculations gives the energetics quantitatively similar to that of CASPT2 and MS-CASPT2. Only M06 family functionals such as M06 and M06-L give the $^5\Pi_g$ state as the ground state; other DFT functionals (hybrid and hybrid-meta) and MP2 predict the $^7\Pi_u$ state as the ground state of $Cr(CO)_2$. Even CCSD(T), a high-level single-reference ab initio method, predicted the $^7\Pi_u$ state as the ground state of $Cr(CO)_2$ in the previous study because its reference wave function is seriously contaminated.[10] These results indicate that the multiconfigurational character of the wave function significantly affects the energetics of $Cr(CO)_2$ as well.

The dependence of the Cr□C and C□O bond lengths of $Cr(CO)_3$ on the computational method is similar to that of $Cr(CO)_2$ except that the Cr□C bond length is underestimated by MP2 instead of being overestimated as in $Cr(CO)_2$. In addition, the energy differences among the states were seriously overestimated by MP2 (see Table S2). Accordingly, MP2 is an inappropriate method for predicting the energetics of transition metal carbonyl complexes. We note that, except M06-L, no DFT functional gives the same energy ordering as CASPT2 predicts. Thus, we conclude that one should be careful in the choice of DFT functional, and GGA or meta-GGA functional may be a better choice than a hybrid one in the system where the multiconfigurational character is not negligible.

CO Stretching Frequency of the $^7\Pi_u$ state

Since the calculation of the Hessian using MS-CASPT2, which gives full numerical Hessian, is quite demanding and impractical, we used DFT and MP2 for the calculation of the vibrational frequencies despite the limitation of these methods in predicting the energetics. Since theoretical methods generally overestimate the C□O stretching frequency, direct comparison between the values from experiment and computation is not relevant. Therefore, certain scaling factors are needed to correct the calculated vibrational frequencies, but they are not available for all DFT functionals at the moment. To circumvent this problem, we considered the ratio of the frequencies of two different vibrational modes instead of the frequency values themselves. First, to find a DFT functional that gives the best agreement

with the experiment, we examined the ratio of the frequencies of an asymmetric (B_2) and a symmetric (A_1) C□O stretching modes for the $^5A_1$ state (bent) because the vibrational frequencies of the $^5A_1$ state are well established experimentally.[13] The experimental values for the ratio (B_2/A_1) of the two frequencies are 0.924 (1821.5 cm^{-1}/1970.8 cm^{-1}) and 0.925 (1832.9 cm^{-1}/1982.1 cm^{-1}) in Ar and Ne matrix environment, respectively.[13] From the calculated frequencies using various functionals (see Table S1), the ratio of the vibrational frequencies for the $^5A_1$ state is determined to be 0.955 (= 1953 cm^{-1}/2044 cm^{-1}, M06-L), 0.927 (= 1936 cm^{-1}/ 2089 cm^{-1}, PBE0), 0.957 (= 2009 cm^{-1}/2099 cm^{-1}, M06), and 1.255 (= 2461 cm^{-1}/1961 cm^{-1}, MP2). Although PBE0 gives the ratios in the best agreement with the experimental values, PBE0 provide peculiarly low values for the C□O stretching frequency of the $^5\Pi_g$ (1704 cm^{-1}) compared with other methods (see Table S1). Therefore, we selected M06 and M06-L DFT functionals for the following comparison. We then check the ratio between the C□O stretching frequencies of the $^5\Pi_g$ and $^7\Pi_u$ states (Σ_u mode of $^5\Pi_g$ / Σ_u mode of $^7\Pi_u$). The ratio of the two frequencies determined from the experimental values is 0.967 (= 1914 cm^{-1} observed by Weitz *et al.*[14] / 1850 cm^{-1} estimated by Andrews *et al.*[13]). The ratio (Σ_u mode of $^5\Pi_g$ / Σ_u mode of $^7\Pi_u$) of the calculated frequencies for the two modes is 0.980 (= 1951 cm^{-1}/ 1990 cm^{-1}, M06-L), which is reasonably close to the experimental value (0.967). In addition, the ratio of M06 is 0.966 (= 1955 cm^{-1}/ 2023 cm^{-1}, M06), which is in excellent agreement with the experimental value (0.967). According to these results, we can conclude that 1914 cm^{-1} mode observed in the transient absorption experiment[14] is not from the C□O stretching of the $^5\Pi_g$ state but from the $^7\Pi_u$ state, supporting the assignment by Andrews *et al.*.[13]

Table S1. The optimized bond lengths of CO and CO^- and the calculated adiabatic electron affinity of CO using (MS-)CASPT2/ANO-RCC-TZ and (MS-)CASPT2/ANO-RCC-QZ.

		Bond Length (in Å)	Electron Affinity (in eV)
CO ($^1\Sigma^+$)	CASPT2/ANO-RCC-TZ	1.129	-2.04[a]
	CASPT2/ANO-RCC-QZ	1.130	-1.91[b]
	[c]MRCI/aug-cc-pVQZ+3 diff. *p*	-	-1.67
	Exp.	1.128	-1.5[d]
CO^- ($^2\Pi$)	MS-CASPT2/ANO-RCC-TZ	1.224	-
	MS-CASPT2/ANO-RCC-QZ	1.220	-
	[c]MRCI/aug-cc-pVQZ+3 diff. *p*	1.210	-

[a]The zero-point energies calculated by PBE0/aug-cc-pVTZ were added.

[b]The zero-point energies calculated by PBE0/aug-cc-pVQZ were added.

[c]The aug-cc-pVQZ with additional three diffuse *p* functions were used, reference 3

[d]Vertical electron affinity, reference 4

Table S2. The optimized geometrical parameters (bond lengths in Å and bond angles in degree), $<S^2>$ values, C□O stretching frequencies (in cm^{-1}), and the relative energies,[a] ΔE (in kcal/mol, including zero-point energy correction, ΔE_{ZPE} in Italic), of the $^3A_2$, $^5A_1$, $^5\Pi_g$, and $^7\Pi_u$ states of $Cr(CO)_2$. The related molecular structures of $Cr(CO)_2$ are shown in Figure 1 in the main text.

$Cr(CO)_2$	M06-L[b]	PBE0	M06	MP2
		$^3A_2/C_{2v}$		
r(Cr□C)	1.812	1.826	1.839	1.866
r(C□O)	1.166	1.160	1.156	1.176
∠CCrC	74.9	74.2	72.5	70.6
∠CrCO	175.5	175.9	175.5	177.1
$<S^2>$	2.235	2.488	2.421	3.644
B_2 (asymm.)	1866	1870	1897	6201
A_1 (symm.)	1995	2026	2037	2737
ΔE, ΔE_{ZPE}	10.7, *11.5*	16.2, *17.2*	13.5, *14.1*	23.3, *31.7*
		$^5A_1/C_{2v}$		
r(Cr□C)	1.977	1.971	2.013	2.003
r(C□O)	1.154	1.148	1.142	1.160
∠CCrC	111.8	110.7	106.7	115.7
∠CrCO	178.3	177.1	179.8	178.6
$<S^2>$	6.465	6.407	6.577	6.820
B_2 (asymm.)	1953	1936	2009	2461
A_1 (symm.)	2044	2089	2099	1961
ΔE, ΔE_{ZPE}	5.3, *4.9*	4.3, *4.3*	1.9, *1.4*	0.8, *0.7*
		$^5\Pi_g/D_{\infty h}$		
r(Cr□C)	1.982	1.980	1.990	1.967
r(C□O)	1.153	1.146	1.144	1.161
Σ_u (asymm.)	1951	1704	1955	2113
$<S^2>$	6.178	6.236	6.222	6.674
ΔE, ΔE_{ZPE}	0.0, *0.0*	0.0, *0.0*	0.0, *0.0*	0.0, *0.0*
		$^7\Pi_u/D_{\infty h}$		
r(Cr□C)	2.033	2.035	2.042	2.030
r(C□O)	1.153	1.145	1.144	1.155
Σ_u (asymm.)	1990	2024	2023	2063
$<S^2>$	12.008	12.009	12.006	12.034
ΔE, ΔE_{ZPE}	6.9, *6.5*	-2.6, *-2.5*	3.2, *2.8*	-14.1, *-14.2*

[a]Relative energies are with respect to the $^5\Pi_g$ state.

[b]The $^7\Pi_u$ state optimized by M06-L has one imaginary frequency (88i cm^{-1}).

Table S3. The optimized geometrical parameters (bond lengths in Å and bond angles in degree), $<S^2>$ values, and the relative energies,[a] ΔE (in kcal/mol, including zero-point energy correction, ΔE_{ZPE} in Italic), of the $^1A_1$, $^3B_1$, $^5B_2$, and $^7A_2''$ states of $Cr(CO)_3$. The related molecular structures of $Cr(CO)_3$ are shown in Figure 1 in the main text.

$Cr(CO)_3$	M06-L[b]	PBE0	M06[b]	MP2[b]
		$^1A_1/C_{3v}$		
r(Cr□C)	1.807	1.801	1.819	1.726
r(C□O)	1.160	1.152	1.150	1.179
∠CCrC	88.5	88.2	88.6	86.2
∠CrCO	178.0	177.8	178.2	177.4
ΔE, ΔE_{ZPE}	0.0, *0.0*	0.0, *0.0*	0.0, *0.0*	0.0, *0.0*
		$^3B_1/C_{2v}$		
r(Cr□C□)	1.900	1.897	1.921	1.892
r(C□□O□)	1.148	1.141	1.139	1.129
r(Cr□C)	1.910	1.902	1.919	1.814
r(C□O)	1.155	1.148	1.147	1.170
∠CCrC	177.7	179.3	177.5	179.9
∠C□CrC	91.1	90.4	91.2	90.1
∠CrCO	178.2	177.2	178.3	178.7
$<S^2>$	2.096	2.114	2.129	2.897
ΔE, ΔE_{ZPE}	9.4, *8.0*	3.3, *2.2*	1.0, *-0.1*	77.9, *76.1*
		$^5B_2/C_{2v}$		
r(Cr□C□)	1.981	1.965	1.987	1.988
r(C□□O□)	1.150	1.144	1.142	1.131
r(Cr□C)	1.989	1.982	1.999	1.939
r(C□O)	1.147	1.139	1.138	1.160
∠CCrC	148.9	155.6	148.2	162.1
∠C□CrC	105.5	102.2	105.9	98.9
∠CrCO	179.5	177.7	179.8	173.2
$<S^2>$	6.119	6.129	6.150	6.670
ΔE, ΔE_{ZPE}	5.7, *3.5*	-5.4, *-7.5*	-7.4, *-9.0*	66.6, *62.9*
		$^7A_2□/D_{3h}$		
r(Cr□C)	2.029	2.037	2.042	2.028
r(C□O)	1.147	1.139	1.138	1.149
$<S^2>$	12.015	12.015	12.009	12.056
ΔE, ΔE_{ZPE}	11.3, *9.0*	-2.4, *-4.9*	-2.8, *-5.0*	50.5, *47.0*

[a]Relative energies are with respect to the $^1A_1$ state.

[b]The $^3B_1$ and $^5B_2$ states optimized by M06-L have one imaginary frequency, 56i cm^{-1} and 22i cm^{-1}, respectively. The $^3B_1$ state optimized by M06 also has one imaginary frequency, 20i cm^{-1}. The $^5B_2$ state optimized by MP2 also has one imaginary frequency, 333i cm^{-1}.

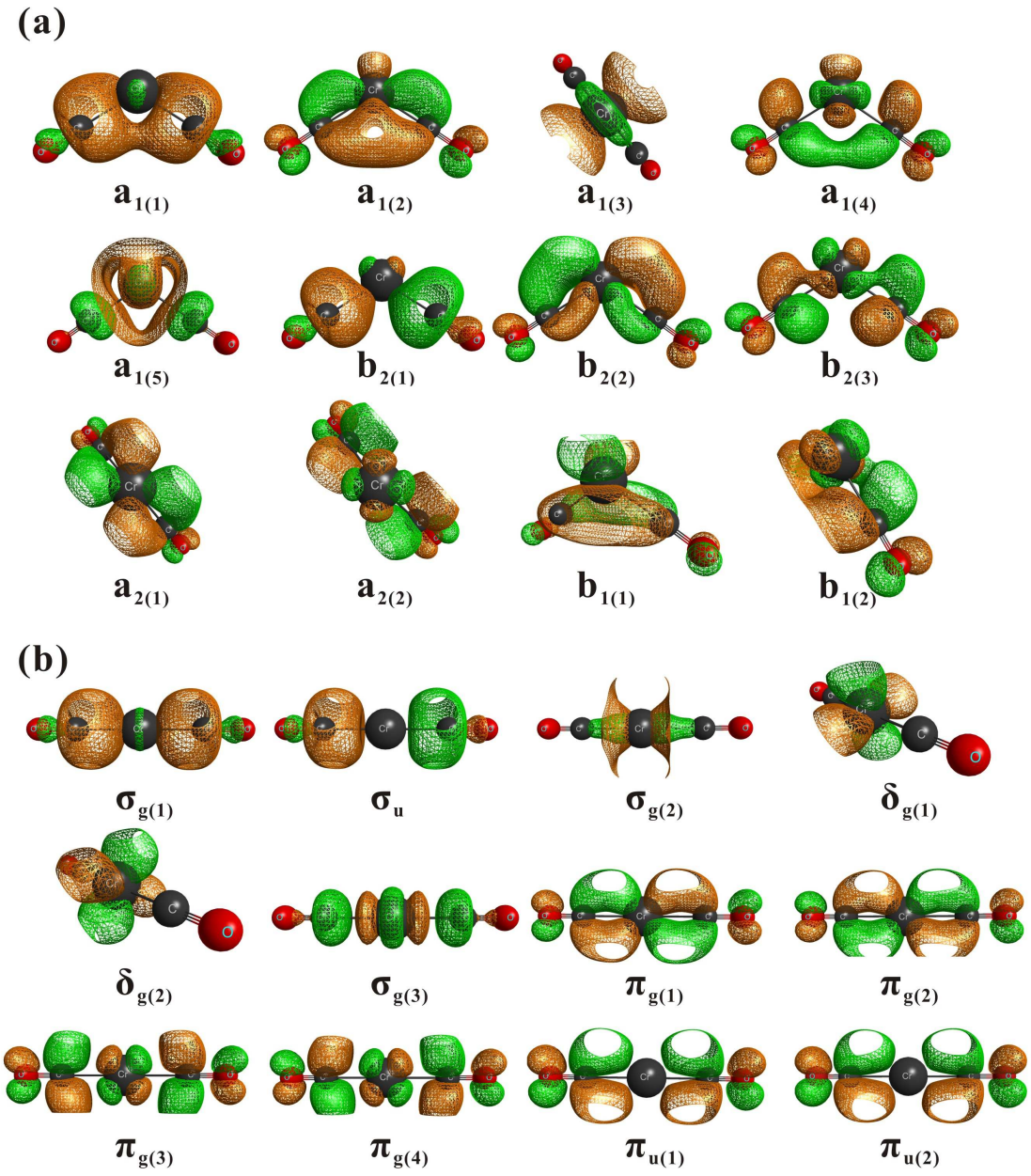

Figure S1. The active orbitals of CAS(10,12) calculations for (a) $^3A_2$ and $^5A_1$ states (bent structures) and (b) $^5\Pi_g$ (^5B) and $^7\Pi_u$ (^7B) states (linear structures) of $Cr(CO)_2$. The related molecular structures are shown in Figure 1 in the main text.

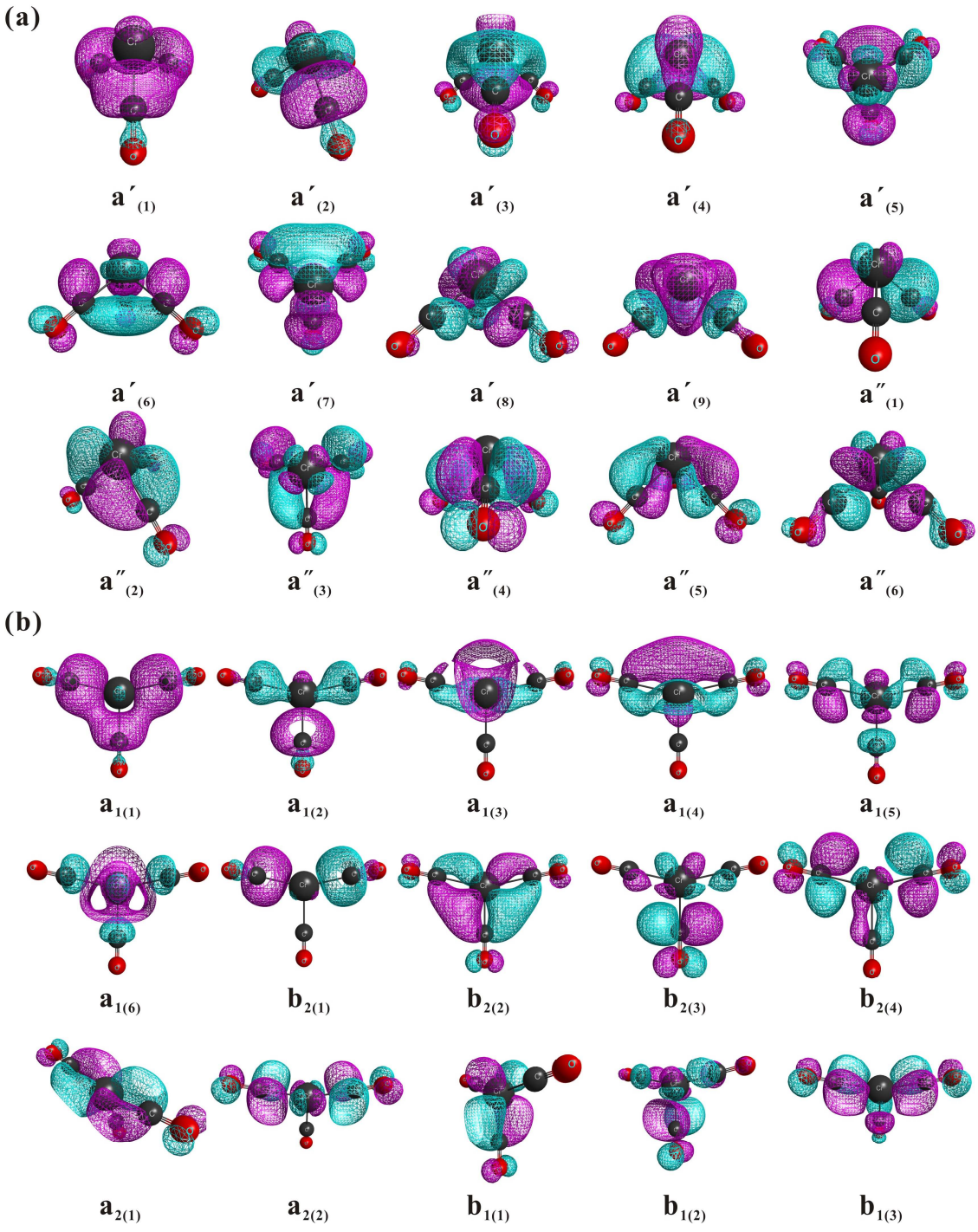

Figure S2. The active orbitals of CAS(12,15) calculations for (a) $^{1}A_{1}$ ($^{1}A\square$) state and (b) $^{3}B_{1}$, $^{5}B_{2}$, and $^{7}A_{2}''$ ($^{7}B_{1}$) states of $Cr(CO)_{3}$. The related molecular structures are shown in Figure 1 in the main text.

References

(1) Refaey, K. M. A.; Franklin, J. L. Endoergic ion—molecule-collision processes of negative ions. III. Collisions of I^- on O_2, CO, and CO_2. *Int. J. Mass Spectrom. Ion Phys.* **1976**, *20*, 19-32.

(2) NIST Chemistry Webbook Site, http://webbook.nist.gov/.

(3) Lee, E. P. F.; Lozeille, J.; Soldan, P.; Wright, T. G. Calculations on the unstable CO^- ($X^2\Pi$) anion. *Chem. Phys. Lett.* **2001**, *336*, 479-487.

(4) Boness, M. J. W.; Hasted, J. B.; Larkin, I. W. Compound State Electron Spectra of Simple Molecules. *Proc. R. Soc. Lond. A* **1968**, *305*, 493-515.

(5) Frisch, M. J.; Head-Gordon, M.; Pople, J. A. Semi-Direct Algorithms for the MP2 Energy and Gradient. *Chem. Phys. Lett.* **1990**, *166*, 281-289.

(6) Head-Gordon, M.; Head-Gordon, T. Analytic Mp2 Frequencies without 5th-Order Storage - Theory and Application to Bifurcated Hydrogen-Bonds in the Water Hexamer. *Chem. Phys. Lett.* **1994**, *220*, 122-128.

(7) Adamo, C.; Barone, V. Toward reliable density functional methods without adjustable parameters: The PBE0 model. *J. Chem. Phys.* **1999**, *110*, 6158-6170.

(8) Zhao, Y.; Truhlar, D. G. The M06 suite of density functionals for main group thermochemistry, thermochemical kinetics, noncovalent interactions, excited states, and transition elements: two new functionals and systematic testing of four M06-class functionals and 12 other functionals. *Theor. Chem. Acc.* **2008**, *120*, 215-241.

(9) Zhao, Y.; Truhlar, D. G. A new local density functional for main-group thermochemistry, transition metal bonding, thermochemical kinetics, and noncovalent interactions. *J. Chem. Phys.* **2006**, *125*, 194101.

(10) Kim, J.; Kim, T. K.; Kim, J.; Lee, Y. S.; Ihee, H. Density functional and ab initio study of $Cr(CO)_n$ (n=1-6) complexes. *J. Phys. Chem. A* **2007**, *111*, 4697-4710.

(11) Balabanov, N. B.; Peterson, K. A. Systematically convergent basis sets for transition metals. I. All-electron correlation consistent basis sets for the 3d elements Sc-Zn. *J. Chem. Phys.* **2005**, *123*, 64107.

(12) Gaussian 09, R. A.1, Frisch, M. J.; Trucks, G. W.; Schlegel, H. B.; Scuseria, G. E.; Robb, M. A.; Cheeseman, J. R.; Scalmani, G.; Barone, V.; Mennucci, B.; Petersson, G. A.; Nakatsuji, H.; Caricato, M.; Li, X.; Hratchian, H. P.; Izmaylov, A. F.; Bloino, J.; Zheng, G.; Sonnenberg, J. L.; Hada, M.; Ehara, M.; Toyota, K.; Fukuda, R.; Hasegawa, J.; Ishida, M.; Nakajima, T.; Honda, Y.; Kitao, O.; Nakai, H.; Vreven, T.; Montgomery, Jr., J. A.; Peralta, J. E.; Ogliaro, F.; Bearpark, M.; Heyd, J. J.; Brothers, E.; Kudin, K. N.; Staroverov, V. N.; Kobayashi, R.; Normand, J.; Raghavachari, K.; Rendell, A.; Burant, J. C.; Iyengar, S. S.; Tomasi, J.; Cossi, M.; Rega, N.; Millam, N. J.; Klene, M.; Knox, J. E.; Cross, J. B.; Bakken, V.; Adamo, C.; Jaramillo, J.; Gomperts, R.; Stratmann, R. E.; Yazyev, O.; Austin, A. J.; Cammi, R.; Pomelli, C.; Ochterski, J. W.; Martin, R. L.; Morokuma, K.; Zakrzewski, V. G.; Voth, G. A.; Salvador, P.; Dannenberg, J. J.; Dapprich, S.; Daniels, A. D.; Farkas, Ö.; Foresman, J. B.; Ortiz, J. V.; Cioslowski, J.; Fox, D. J. Gaussian, Inc., Wallingford CT, 2009.

(13) Andrews, L.; Zhou, M. F.; Gutsev, G. L.; Wang, X. F. Reactions of laser-ablated chromium atoms, cations, and electrons with CO in excess argon and neon: Infrared spectra and density functional calculations on neutral and charged unsaturated chromium carbonyls. *J. Phys. Chem. A* **2003**, *107*, 561-569.

(14) Seder, T. A.; Church, S. P.; Weitz, E. Wavelength dependence of excimer laser photolysis of $Cr(CO)_6$ in the gas phase. A study of the infrared spectroscopy and reactions of the $Cr(CO)_x$ (x = 5, 4, 3, 2) fragments. *J. Am. Chem. Soc.* **1986**, *108*, 4721-4728.